Geometric Model of Concrete at Mesoscale –Parameters, Shape Description and Generation Strategies

Conference Paper · June 2021

CITATIONS
0

READS
163

3 authors:

Qifan Ren
University of Lisbon
20 PUBLICATIONS **177** CITATIONS
SEE PROFILE

João Pacheco
c5Lab - Sustainable Construction Materials Association
44 PUBLICATIONS **1,197** CITATIONS
SEE PROFILE

Jorge de Brito
University of Lisbon
1,676 PUBLICATIONS **41,239** CITATIONS
SEE PROFILE

Geometric Model of Concrete at Mesoscale - Parameters, Shape Description and Generation Strategies

Qifan Ren[1], João Pacheco[2,*], Jorge de Brito[3]

1. PhD Candidate, CERIS/ Instituto Superior Técnico, Universidade de Lisboa, Lisbon, Portugal
2. Researcher, CERIS/ c[5]Lab, Sustainable Construction Materials Association, Lisbon, Portugal
3. Full Professor, CERIS/ Instituto Superior Técnico, Universidade de Lisboa, Lisbon, Portugal

[*]Corresponding author email: joaonpacheco@tecnico.ulisboa.pt

Abstract

To facilitate the assessment of concrete mix design and of its mechanical behaviour, numerical modelling techniques at meso-scale are currently being popularized as a valuable tool in materials and structural engineering. Generally, the structure of concrete at the mesoscale model is recognized as a three-phase heterogeneous material consisting of coarse aggregates, mortar matrix, and interfacial transition zones (ITZ). A successful computational model to study the heterogeneous concrete requires not only accurate mechanical modelling, but also a realistic representation of the mesoscale geometry of concrete. The aims of this paper are to identify relevant parameters for geometric modelling as well as generation strategies of mesoscopic phases for future coupling with a numerical model for mechanical simulations. This review argues that mesoscale model should consider the properties of aggregates e.g. shape, particle size distribution, volumetric fraction of coarse aggregate, and three features of concrete specimens - ITZ, size effect, and wall effect. Reference values and methods for modelling those parameters are assessed from the literature. The state-of-the-art of generation of mesoscopic phases is presented in terms of generation of aggregate, overlapping detection and generation of ITZ. Emphasis is given on a more adaptable method - random aggregate model - and relevant approaches are listed. Several strategies are proposed to limit the number of aggregates to be checked for overlapping detection, including identification of neighbouring particles, circumscribed spheres, and bounding box. Four popular methods for the generation and placement of aggregates are presented, each with its own merits. Based on the analysis of current literature on this topic, recommendations for mesoscale modelling are made and an example of their application is presented. It is argued that future developments of the proposed geometrical model should treat the calibration of parameters based on specific experiments.

Keywords: *Geometric model, concrete, mesoscale modelling, overlapping detection, ITZ generation.*

1. Introduction

Experimental testing requires significant amounts of time and energy to evaluate a concrete mix design, especially in the case of mix design optimization and when studying concrete with incorporation of new, unconventional, materials. To facilitate the assessment of concrete mix design and its mechanical behaviour, numerical modelling techniques at the mesoscale are currently being popularized as a valuable tool in both material and mechanical engineering. Mesoscale models can explicitly simulate the macroscopic stress-strain relationship, estimating stress-paths, strains, damage and crack progression (Carrara et al. 2018). Therefore, mesoscale models analyse the phenomenological causes of mechanical failure, allowing understanding the limiting factors e.g. determine the limiting mesoscale phase (either the coarse aggregates, the mortar matrix, or the interfacial transition zone between coarse aggregates and mortar - ITZ) that prevents a concrete mix from reaching its intended performance.

Concrete is a multi-phase artificial material, composed of a cementitious matrix and fine aggregates (which form a mortar matrix), coarse aggregates, and ITZ between the coarse aggregates and the mortar matrix in the mesoscale modelling (Carrara et al. 2018) (Zhang et al. 2017). A successful computational model to study the behaviour of a concrete specimen requires that the mesoscale geometry of concrete is realistically simulated, that input parameters for the behaviour of coarse aggregates, mortar, and ITZ

are selected, and that meshes and finite elements are defined.

This paper reviews the geometric modelling of the mesoscale of concrete in terms of parameters needed and strategies to generate the mesoscopic phases. Due to the complex nature of concrete, mesoscopic modelling is a trade-off of realistic representation against implementation cost. With this idea in mind, recommendations for modelling are presented and an example of their application is provided.

2. Parameters needed for geometrical modelling

This section is focused on the parameters that are relevant for coarse aggregates modelling, since all mesoscopic models represent coarse aggregates explicitly and consider fine aggregates as part of mortar (Okan and Molinari 2017) (Thilakarathna et al. 2020a). Fine aggregates are included in mortar since their explicit generation and meshing implies very large computational costs.

2.1. Properties of aggregates

The shape of aggregates is relevant not only for the fresh-, but also for the hardened-state behaviour of concrete. Amongst other aspects, the stress necessary for micro-crack initiation and development along the surface of aggregates is associated with the shape of the aggregates and the strength of the ITZ is affected by their roughness. Mesoscale models generally simulate particles by assuming one of three shapes: i) in 2D modelling: circular, elliptical, or polygonal (Wang, Kwan and Chan 1999); II) in 3D modelling: spherical (Wriggers and Moftah 2006), ellipsoidal (Häfner et al. 2006), or polyhedral (Zhang et al. 2017). Circular/spherical or elliptical/ellipsoidal (Figure 1) aggregates can be easily simulated with high computational efficiency in a Cartesian space through their parametric equations. With the improvement of computation power, research on more realistic geometric modelling for aggregates is ongoing, e.g. using polyhedrons. These can be generated through methods such as the convex hull algorithm (Zhou et al. 2017), the convex extension of a spherical particle (Ma, Xu and Li 2016), or the non-convex polyhedron generation method (Meng, Lv and Liu 2020). However, algorithms based on complex shapes have two limitations: i) computational cost and ii) ambiguity in the experimental measurement, parametrization, and computational representation of particles with complex shape. Therefore, ellipsoids still play an important role in mesoscale modelling due to computational efficiency and adequate measurement in real particles and computational representation with clearly-defined and non-ambiguous parameters (the axes of ellipses).

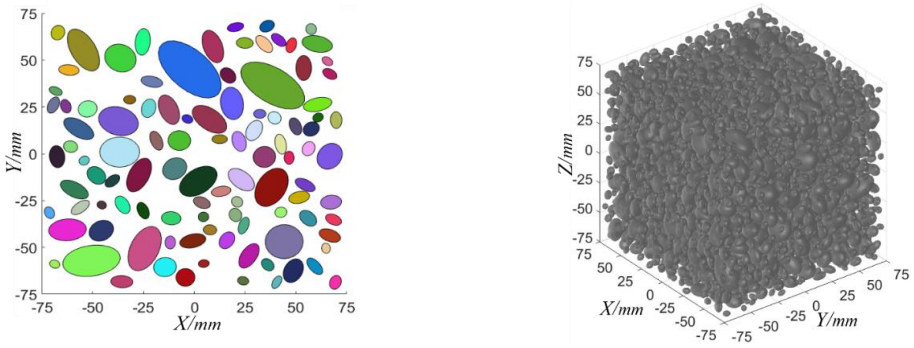

(a) Elliptical aggregates (b) Ellipsoidal aggregates

Figure 1. Geometrical models in 2D and 3D.

Another approach is to build mesoscale models using the shape (and location) of aggregates as analysed from actual concrete specimens. This is made through photographs of the samples and imaged-detection algorithms in 2D modelling, or using X-ray computed tomography in 3D implementations of mesoscale modelling. This approach is outside the scope of this paper, since it aims at developing a mesoscale model that will be used in the future for predictive applications (for concrete mix design optimization without producing every mix design simulated).

The particle size distribution of the aggregates of a mix design governs packing and voids content, as

well as the mechanical properties of concrete since it plays an important role on the mode of failure and on crack branching (van Mier 2017). The larger the maximum aggregate size, the more heterogeneous the mix becomes and the smaller the aggregate size, the less porous the ITZ is, resulting in a stronger and less micro-crack susceptible ITZ (Alexander 2005). The Fuller grading curve is widely used in mesoscale modelling to define the size distribution of particles, due to its simplicity and convenience (Zhang et al. 2019), but when simulating the mesoscale behaviour of a concrete mix design, the real grading curve of the mix design should be used, even if this requires sieving the aggregates that will be used for the concrete mix under optimization (Gatuingt et al. 2013).

The volumetric content of the aggregates has an important influence on the mechanical behaviour of concrete, since it influence stress paths, crack propagation and fracture energy, as well as stiffness and stress and strain distribution between mortar and aggregates. Wriggers and Moftah (2006) argue that, for most concrete compositions, coarse aggregates occupy around 40–50% of concrete's volume. In most publications on the mesoscale modelling of concrete, the volumetric content of coarse aggregates is between 30% and 50% (Thilakarathna et al. 2020b) (Xu, Lv and Chen 2013) (Okan and Molinari 2017).

2.2. Interfacial transition zone

The ITZ is commonly the weakest phase of conventional concrete since, due to micro-bleeding around the surface of the aggregates, ITZs are more porous, weaker and more deformable than both aggregates and mortar (Scrivener et al. 2004) From this reasoning follows that an accurate simulation of the characteristics of the ITZ (namely thickness, strength and elasticity) improves the accuracy of mesoscale simulations.

The ITZ thickness is accepted to be in the range of 10 μm to 50 μm (Mehta and Monteiro 2006) . However, defining the layer of the ITZ with a realistic thickness (10~50 μm) will result in drastic loss of computational efficiency of numerical models due to the very large number of finite elements required (Thilakarathna et al. 2020a). A feasible solution is using an equivalent layer with relative higher thickness to represent real ITZ, i.e. enlarge the thickness to some extent. More details on modelling approaches of ITZ are presented in a later section of the paper.

2.3. Size effect and wall effect

Size effect is caused by energy-related and statistical phenomena (Bažant and Yavari 2005). The former can be captured with fracture mechanics approaches, yet the latter requires that material properties consider material heterogeneity. Statistical size effect is addressed in the numerical model as long as the specimen is larger than the representative volume element (RVE) - which is the smallest volume over which a measurement of a property of a composite, heterogeneous, material is representative of the overall specimen (Dubey and Noshadravan 2020). Random material properties are attributed to the mesoscale elements and the mesoscale elements are randomly placed in RVEs. Conventionally, RVEs require that the size of the specimen is at least 3-5 times the maximum aggregate diameter (Okan and Molinari 2017). Thus, numerical applications of mesoscale modelling are commonly made in cubic specimens with 100 mm edges (Wriggers and Moftah 2006) (Han et al. 2016) (Meng, Lv and Liu 2020), which comply with this criterion for concrete with common maximum aggregate diameter (16 to 25 mm) (Gatuingt et al. 2013) (Wriggers and Moftah, 2006). Energy-related size effects may be accounted for using fracture mechanics (Bazant 2005).

Wall effect is a physical phenomenon that affects the placement of aggregate within concrete elements. Wall effect may be separated in two types: the trend for larger particles being located away from the concrete surface and the trend for large particles being closer to small particles and distant from other large particles. Based on previous research, Wang et al. (1999) and Wriggers and Moftah (2006) modelled both types of wall effect as minimum distances. Equation (1) models the minimum distance between a particle and the concrete surface, while (2) models the minimum distance between particles.

$$D_1 = \gamma \times d \tag{1}$$

$$D_2 = \gamma \times \min\{d_A, d_B\} \tag{2}$$

In these equations, γ is a distribution factor related to aggregate volume content. The value of γ has a considerable influence on the spatial distribution of the aggregate. Wriggers and Moftah (2006) determined

an iterative value for γ using an algorithm that starts with a large γ that decreases iteratively when part of the aggregate particles of a concrete mix design cannot be placed on the concrete specimen due to lack of space. This concept agrees with the notion that the particles of mixes with large coarse aggregate content are more closely packed, yet the experimental validation of values for γ is lacking.

2.4. Grading and mesoscale modelling

The volume content of the constituents of the simulated concrete should be equal to that of the mix design of the real concrete mix. However, the way grading curves are defined must be considered when developing a mesoscale geometrical model. Grading is defined in terms of the total mass of particles that corresponds to a size interval and algorithms for aggregate generation need to convert this information into the number of particles of that size interval. This is achieved through the density, dimension, and volume of the particles.

When either real grading or a theoretical grading curve is used, it must be considered that the dimension of 3D particles is represented by thickness, width, and length, but the grading curve is defined in terms of particle diameter only. This diameter is defined in terms of an interval of sieves with opening *d/D*, which is a range of values of size that the particles may have. Mesoscale models need to: 1) distribute particles within the range of widths possible of a sieve interval; ii) relate the admissible interval *d/D* with the geometry of the particle being generated. Alternative methods to relate the dimension of virtual particles with grading diameter are based on the shape used to model the particles. Some authors use the equivalent diameter D_{eq} to describe diameter of irregular particles, such as Xu, Lv and Chen (2013) who defined D_{eq} as the diameter of a sphere with the same volume of the particle. Xu and Chen (2013) presented the D_{eq} of both ellipsoids and several types of polyhedral particles.

3. Generation of mesoscopic phases

3.1. Generation of aggregates

A random aggregate structure (RAS) defines shape, volume fraction, grading, and spatial position of the coarse aggregate (Wang, Kwan and Chan 1999). According to the basic principle of the numerical mesoscale building process, there are four frequently used method to reproduce the geometric configuration: the Voronoi graphic method (Zhang et al. 2019), image-based methods (Carrara et al. 2018), local background grid method (Meng et al. 2020) and random aggregate model (RAM) (Wang, Kwan, and Chan 1999).

The RAM has been increasingly used and was originally developed by Wittmann et al. (1985). This model combines two procedures: (i) the random generation of the geometry of the aggregate particles; (ii) the random placement of the particles within the concrete specimen by defining their location and rotation. During placement, overlapping detection algorithms check whether particles are overlapping. The random location and rotation of the particles is made with Monte Carlo Simulation.

Within the framework of RAM, a series of methods has been developed to build RAS, but each method places the particles using different algorithms. Moreover, the initial parameters needed for the geometrical modelling differ from method to method. A list of methods and corresponding references are: take-and-place method (Wang, Kwan and Chan 1999), random dropping method (Van Mier and Van Vliet 2003), take-and-place regeneration method (Wriggers and Moftah 2006), random packing method (Xu and Chen 2013), occupation and removal method (Ma, Xu and Li 2016), random walking method (Zhang et al. 2017), and enhanced take-and-place method (Zhou et al. 2017).

The packing capacity varies between approaches used for mesoscale modelling and this should be accounted for when choosing a packing method. For example, the take-and-place method can pack aggregate particles roughly up to 40% of the total volume with a reasonable computational time (Thilakarathna et al. 2020b), while the Voronoi graphic method can easily pack fairly high volume fractions, but with gradual loss of verisimilitude to real concrete (Karavelić et al. 2019).

3.2. Overlapping detection

When placing aggregates in a concrete volume, the model requires that: 1) aggregate particles be entirely inside the boundary of the concrete specimen; 2) particles do not overlap. In these verifications, the two types of wall effect are also considered by imposing that the overlapping checks include the minimum distance requirements D_1 and D_2 presented in (1-2) - in practical terms, the boundaries of the particles are artificially enlarged during overlapping detection. Requirement 1) is checked by verifying whether any vertex of a particle is outside the boundary defined by the specimen's dimensions and wall effect D_1. If MATLAB is used, functions *inpolygon* - in 2D, or *inpolyhedron* - in 3D, may be used.

As for requirement 2), overlapping between two particles may be determined by the central distance if the particles circular or spherical. If the shape of the particles is elliptical or ellipsoidal, their equations may be used to check whether the vertices of ellipse or ellipsoid $\mathcal{A}$ is inside $\mathcal{B}$ (Figure 2a). Before detection, Zhang et al. (2017) check whether the particle being placed is nearby any already-placed particle and only check overlapping for particles that are near. For ellipsoids, Häfner et al. (2006) developed an advanced two-step algorithm: (i) checking whether bounding boxes (dashed lines in Figure 2a) of the two particles are separated; (ii) If not, a further check is made based on the characteristic equation $f(\lambda) = \det(\lambda\mathbf{A} + \mathbf{B})$ of the two ellipsoids denoted by matrix form **A** and **B**. If Equation $f(\lambda)$ has two distinct positive real roots, the ellipsoids do not intersect.

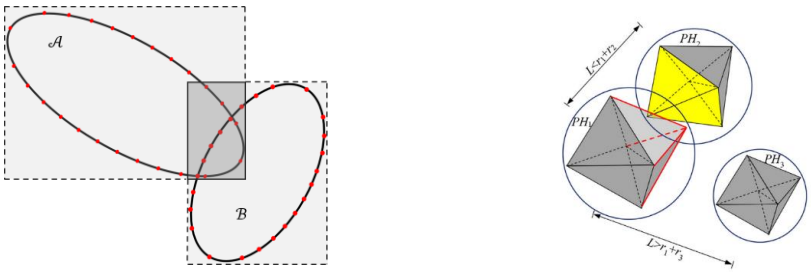

(a) (b)

Figure 2. Intersection check based on (a) bounding box; (b) circumscribed spheres (Zhang et al. 2017).

Overlapping detection is very challenging in the case of polygons and polyhedrons. Häfner et al. (2006) presented three approaches for separation check of polygons and polyhedrons: pointwise separation checks within overlapping bounding boxes, division in sub-domains, and grid-based separation checks (Ma, Xu and Li 2016) on the complete domain. Zhou et al. (2017) represents virtual polyhedrons by circumscribed spheres and identifies neighbouring particles of the particle being placed, as shown in Figure 2b. Subsequently, a clipping and capping algorithm is used to further detect the potential overlap. Based on the MATLAB functions (*inpolygon* and *inpolyhedron*) and the concept of circumscribed spheres, Zhang et al. (2017) developed a similar strategy with six steps.

3.3. Generation of mortar and ITZ

Generally, the ITZ may be represented (Thilakarathna et al. 2020) by either of: (1) a thin layer surrounding the aggregate particles; (2) a zero-thickness element used to simulate the mechanical behaviour of ITZs in finite element model. This review focuses on the modelling of the ITZ by a thin layer. There are four types of approaches with different procedure.

The solid layer approach uses an equivalent layer with relative higher thickness to represent real ITZ i.e. enlarge the thickness to some extent. The solid layer is a thin shell around aggregates that represents the ITZ (Figure 3) (Zhou et al. 2017). The layer can be determined by either shrinkage or expansion of the geometry of aggregates. The former decreases the size of the aggregates (changing the particle size distribution to smaller particles), while the latter decreases the volume of mortar (which is conceptually more accurate). The solid layer approach assumes that the ITZ is a uniform shell that surrounds each aggregate concentrically (Xu and Li 2017). In other words, the thickness of the ITZ of each particle is uniform. Yet ITZ for different particles may have with different thickness, if the model defines thickness as dependent on particle size.

The equivalent solid layer approach generates an equivalent ITZ layer after the initial meshing of the mortar domain. This is achieved by identifying the mortar elements that are in contact with the aggregates (Zhou et al. 2017) and considering that these elements are the ITZ. The thickness of ITZ created with this method is mesh-dependent.

Pixel- or voxel-based methods assume that pixels/voxels that are adjacent to aggregates are the ITZ. As a result, the ITZ around aggregates is modelled as a layer with a one-pixel/voxel thickness (Liu et al. 2018).

The aggregate-expansion method proposed by Li and Li (2015) assumes a more realistic thickness for the ITZ. This method imports the finite elements of the surface of particles and performs an expansion of 50 μm. The geometry of the expansion area then is meshed in ABAQUS with wedge elements to represent the ITZ. The remaining volume (the total volume except aggregates and ITZs) serves as mortar phase, which is meshed subsequently in the finite element packages after geometric meso-structure generation.

3.4. Recommendations for geometrical modelling

The philosophy for recommendations is to properly balance the computational cost and realistic representation of concrete meso-structure. Among all shape description approaches for the representation of 3D aggregate particles, ellipsoids are recommended since they adequately represent the shape of real aggregates and their modelling is computationally efficient in comparison to polyhedrons. Moreover, their shape is defined by the length of three orthogonal axes, which may be non-ambiguously measured on aggregate particles and be estimated from shape index and flakiness. It is recommended that the ITZ is modelled through a solid layer approach surrounding aggregates since its application is computationally-efficient and its influence on the numerical modelling of mechanical properties is negligible (Song and Lu 2012). The take-and-place method is suggested to build the meso-structure of concrete specimens since it can randomly place particles in the specimen volume from large to small one by one continuously until reaching the designated volume fraction of aggregates, as well as can define geometrical parameters for each individual particle. Moreover, this method can be readily adapted with the recommendations presented in Section 4. Nevertheless, concerning the packing ability, researchers should determine the packing method according to volume fraction and research purpose. Overlapping detection is advised to identify the neighbouring particles as a preliminary check using circumscribed spheres and use the characteristic equation $f(\lambda) = \det(\lambda A + B)$ for a further check.

4. Improved model and demonstrative application

The application of a geometrical model under development is now presented. The method adopts all recommendations stated in the last section, as well as other techniques that improve computational efficiency e.g. linear transformation methods and matrixial-form checks used for particle overlap detection. Figure 4 illustrates the diagram with the steps of the method.

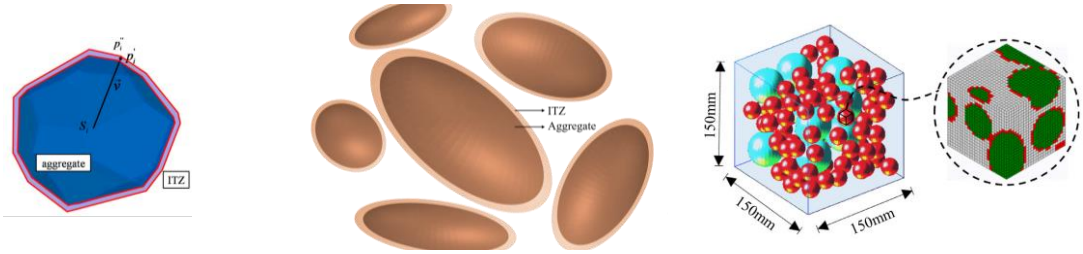

(a) (b) (c)

Figure 3. Schematic diagram of (a) generating ITZ (Zhang et al., 2019; (b) ellipsoidal aggregates with ITZs and space between particles; (c) visualization of the geometrical model) (Jin et al. 2018).

Step 1 is the transformation of sieve openings into the dimensions of particles and is needed because grading curves are defined in terms of the width of aggregates only. Therefore, the length and thickness of particles need to be randomly defined from the width, based on appropriate probability models developed from the characteristic of the aggregates to be used (flakiness category (EN 206 2013)) that

may be complemented with information from a specific testing made on a batch of these aggregates (e.g. shape index (EN 933-4 2008) and flakiness (EN 933-3 2012)). Step 2, the number of aggregates to be generated and placed, is determined from the volume and density of individual ellipsoids.

The third step defines the size of particles represented by standard ellipsoid in matrix form. Standard ellipsoids are defined in Cartesian coordinates by:

$$\left(\frac{x}{R_x}\right)^2+\left(\frac{y}{R_y}\right)^2+\left(\frac{z}{R_z}\right)^2=1 \tag{3}$$

where R_x, R_y, and R_z are the principal semi-axes of the ellipsoid in axes X, Y, and Z. In a matrixial form, the representation of ellipsoids is (Alfano and Greer 2003):

$$\boldsymbol{X}^T\boldsymbol{S}\boldsymbol{X}=0 \tag{4}$$

where $\boldsymbol{X}$ represents a point in 3D space, herein formed by a four-dimensional position vector:

$$\boldsymbol{X}=[x\ y\ z\ 1]' \tag{5}$$

After the geometry of the ellipsoid is randomly-generated, the ellipsoid is randomly rotated and translated (step 4) using two separate matrices: rotation matrix $\boldsymbol{R_o}$ and translation matrix $\boldsymbol{T}$. Coordinates of the point for $\boldsymbol{X}$ after transformation are:

$$\boldsymbol{X}^*=\boldsymbol{T}\boldsymbol{R_o}\boldsymbol{X} \tag{6}$$

Therefore, the matrix representation of a general ellipsoid after random generation, translation and rotation is derived from (4) and (6):

$$\boldsymbol{X}^{*T}\boldsymbol{U}^T\boldsymbol{S}\boldsymbol{U}\boldsymbol{X}^*=0 \tag{7}$$

where $\boldsymbol{U}=\boldsymbol{R_o}^{-1}\boldsymbol{T}^{-1}$ represents the rotation and translation operators and $\boldsymbol{U}^T\boldsymbol{S}\boldsymbol{U}$ is the characteristic matrix of the general ellipsoid after the random rotation and translation (step 5).

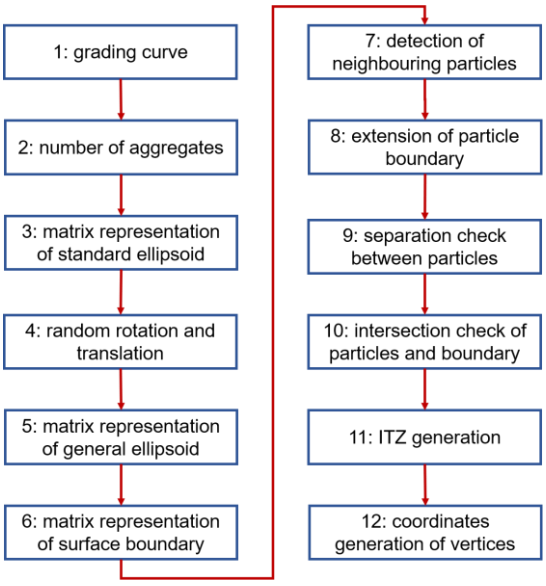

Figure 4. Diagram of all steps of the method.

Step 6 concerns the production of the matrix that represent the surface boundaries of the specimen and this step is needed for the overlapping detection algorithm. In this step, the surfaces of the concrete specimen that is being simulated are defined as planes in algebraic form ($Gx+Hy+Jz+K=0$) and these equations are rewritten following the same matrix form of the ellipsoids, see (4).

Step 7 determines neighbouring particles of the new-generated particle, as depicted in Figure 2(b), in order to limit the total number of particles to be checked for overlap between particles in step 9. Step 8 is the extension of the boundary of particles for overlapping detection to account for distance

requirements (D_1 and D_2). It is noted that D_2 in (2) is not a constant value for the new-generated particles but depends on the minimum diameter of the pairs of particles being checked (the pairs are defined as the particle being placed and each of its neighbouring particles). A scaling matrix is used to accomplish the operation, defining the how much is scaled in three axes.

Then, step 9 uses an analytical method developed by Alfano and Greer (2003) to detect the overlapping between aggregates, or aggregates and boundary. Given two arbitrary ellipsoids $\mathcal{A}$ and $\mathcal{B}$:

$$\boldsymbol{X}^T \boldsymbol{A} \boldsymbol{X} = 0 \tag{8}$$

$$\boldsymbol{X}^T \boldsymbol{B} \boldsymbol{X} = 0 \tag{9}$$

multiplying a scalar constant λ to (8) and subtracting (9) yield:

$$\boldsymbol{X}^T (\lambda \boldsymbol{A} - \boldsymbol{B}) \boldsymbol{X} = 0 \tag{10}$$

After manipulation, (10) becomes:

$$\boldsymbol{X}^T \boldsymbol{A} (\lambda \boldsymbol{I} - \boldsymbol{A}^{-1} \boldsymbol{B}) \boldsymbol{X} = 0 \tag{11}$$

$\boldsymbol{A}^{-1}\boldsymbol{B}$ is the characteristic matrix representing degenerate quadric surfaces and λ stands for the eigenvalue of $\boldsymbol{A}^{-1}\boldsymbol{B}$. Alfano and Greer (2003) found that two negative distinct real eigenvalues occur when ellipsoids $\mathcal{A}$ and $\mathcal{B}$ separate. The method just described is also used to determine the intersection between ellipsoid and surface boundary by substituting $\boldsymbol{A}$ and $\boldsymbol{B}$ with the matrix representation of the ellipsoid and the surface plane (Step 10).

Afterwards, step 11 generates the ITZ. The boundary of the surface of the ITZ boundary is generated by extending the surface of aggregates. The scaling matrix is defined from the ITZ thickness to calculate the matrix representation matrix of ITZ boundary.

At this point, the mesoscale model is built. All information about the model - radii, rotation angle, and central location of each particle, has been stored in a series of matrices. The coordinates of the surface boundary of the particles and ITZs may be readily computed based on these matrices (step 12).

An example of the application of the model is illustrated in Figure 5. The model uses the experimental concrete mix design presented in Pacheco et al. (2019) for the mix labelled as REF. The geometric model concerns a cube with edges of 150 mm. The total weight of aggregate per unit volume of concrete and apparent density of coarse aggregates are 1141 kg/m^3 and 2670 kg/m^3, respectively. The volume fraction of coarse aggregate is 42.73%. The diameter of coarse aggregates ranges from 4 mm to 22.4 mm. The thickness of ITZ is assumed as 200 μm.

Table 1 lists the mean (m) and standard deviation (s) of outputs of the model after ten runs of the algorithm for each segment of particle sizes, including volume fraction, running time, mean diameter, and number of aggregates. Running time is the time between the start of the algorithm and the generation of the coordinates of the surface vertices of the last aggregate.

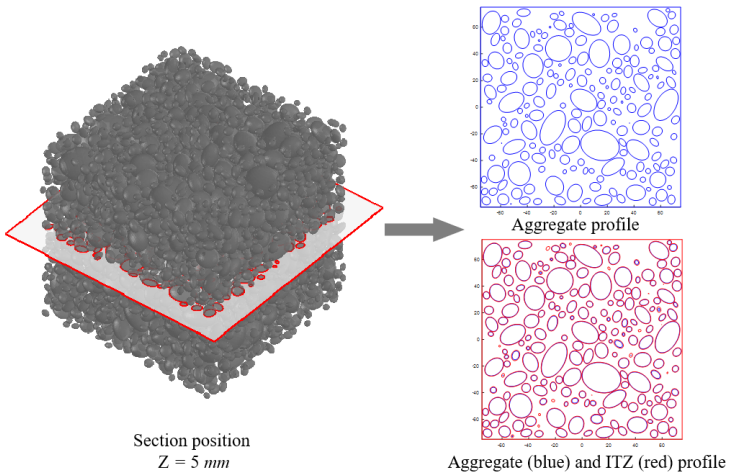

Figure 5. 2D sections of the 3D model.

Table 1 Information in each segment of the model.

Segment	Volume fraction/%		Running time/s		Number of aggregates		Mean diameter/mm	
	m	*s*	*m*	*s*	*m*	*s*	*m*	*s*
1(16~22.4mm)	8.94	0.09	0.02	0.01	39	2.28	19.00	0.20
2(11.2~16mm)	15.77	0.09	2.10	0.45	252	5.66	12.77	0.07
3(8~11.2mm)	6.77	0.01	5.90	0.43	343	5.28	8.88	0.03
4(5.6~8mm)	5.26	0.01	13.73	1.08	752	10.11	6.26	0.02
5(4~5.6mm)	6.00	0.00	144.90	10.52	2447	22.04	4.43	0.01
Total(4~22.4mm)	42.73	0.00	166.65	11.83	3833	34.14	/	/

The results presented in Table 1 are compared with those of a common algorithm, based on an aggregate placing algorithm developed by Wriggers and Moftah (2006) and on the overlapping detection method of Zhang et al. (2017). The comparison checks the computational efficiency of the algorithm developed in this paper; therefore, the two algorithms were run on the same hardware (Intel Core i5-10210U 2.11GHz, RAM 8GB, disk write speed 1737.52 MB/s) and operating system (64-bit Windows 10). With same initial parameters, the traditional program requires 23501.35 s to pack 4861 coarse aggregates, while the method in this paper builds the model in approximately 165 s. As understood from the comparison, the model presented in this paper is significantly faster but places less particles. Future research by the authors will compare the predictions of the model they proposed with the meso-structure of actual concrete specimens to check whether the parameters presented in Table 1 are confirmed.

5. Conclusion

This paper presented parameters needed for geometrical modelling and generation strategies of mesoscopic phases. An improved method combining the methods deemed as the most appropriate after a review of different strategies was stated. The conclusions are that: 1) mesoscale modelling should consider the shape, grading, and volume content of coarse aggregates as well as ITZ and wall effect, but fine aggregates may be assumed as part of mortar; 2) wall effects may be divided in two types and properly simulated with a distribution factor and an iterative process while conducting overlapping detection; 3) the two-step strategy - identification of the particles near the newly-generated particle and separation check - is recommended to detect overlapping; 4) considering ITZ as a thin layer is the most acceptable method to date and this may be achieved through different approaches (solid layer approach, equivalent solid layer approach, and aggregate expansion approach); 5) the improved method proposed can improve the computational efficiency and obtain a realistic geometric representation of concrete specimen.

Future research should focus on including shape and flakiness index in mesoscale modelling since these parameters are widely used to assess the characteristics of the aggregates. Besides, wall effect has not been fully validated with experimental observations in the mesoscopic models.

6. Acknowledgements

The first author greatly acknowledges the China Scholarship Council for the financial support for his PhD research [Grant number: 201906370013]. The CERIS research centre is also acknowledged.

7. References

Alexander, M. (2005). Aggregates in Concrete. Taylor & Francis, Lodon and New York.

Alfano, S., Greer, ML. (2003). Determining if two solid ellipsoids intersect. Journal of Guidance, Control, and Dynamics, 26, 106–110.

Bazant, ZP. (2005). Scaling of structural strength. Elsevier/Butterworth-Heinemann, Oxford, Burlington, MA.

Bažant, ZP., Yavari, A. (2005). Is the cause of size effect on structural strength fractal or energetic-statistical? Engineering Fracture Mechanics, 72, 1–31.

Carrara, P. et al. (2018). Improved mesoscale segmentation of concrete from 3D X-ray images using contrast enhancers. Cement and Concrete Composites, 93, 30–42.

Dubey, V., Noshadravan, A. (2020). A probabilistic upscaling of microstructural randomness in modeling mesoscale elastic properties of concrete. Computers & Structures, 237, 1-14.

EN 206, 2013. Concrete: Specification, performance, production and conformity. Incorporating corrigendum May 2014.
EN 933-3, 2012. Tests for geometrical properties of aggregates. Determination of particle shape. Flakiness index.
EN 933-4, 2008. Tests for geometrical properties of aggregates. Determination of particle shape. Shape index.
Gatuingt, F., Snozzi, L., and Molinari, J. (2013). Numerical determination of the tensile response and the dissipated fracture energy of concrete: role of the mesostructure and influence of the loading rate. International Journal for Numerical and Analytical Methods in Geomechanics, 37, 3112–3130.
Häfner, S. et al. (2006). Mesoscale modeling of concrete: Geometry and numerics. Computers & Structures, 84, 450–461.
Han, D. et al. (2016). Verification and application of two-dimensional slice identification method in three-dimensional mesostructure under different aggregate gradations and packing algorithms. Construction and Building Materials, 102, 843–851.
Jin, L. et al. (2018). Determination of the effect of elevated temperatures on dynamic compressive properties of heterogeneous concrete: A meso-scale numerical study. Construction and Building Materials, 188, 685–694.
Pacheco, J.et al. (2019). Experimental investigation on the variability of the main mechanical properties of concrete produced with coarse recycled concrete aggregates. Construction and Building Materials, 201, 110–120.
Karavelić, E. et al. (2019). Concrete meso-scale model with full set of 3D failure modes with random distribution of aggregate and cement phase. Part I: Formulation and numerical implementation. Computer Methods in Applied Mechanics and Engineering, 344, 1051–1072.
Li, S., Li, Q. (2015). Method of meshing ITZ structure in 3D meso-level finite element analysis for concrete. Finite Elements in Analysis and Design, 93, 96–106.
Liu, C. et al. (2018). Numerical modelling of elastic modulus and diffusion coefficient of concrete as a three-phase composite material. Construction and Building Materials, 189, 1251–1263.
Ma, H., Xu, W., and Li, Y. (2016). Random aggregate model for mesoscopic structures and mechanical analysis of fully-graded concrete. Computers & Structures, 177, 103–113.
Mehta, PK., Monteiro, PJM. (2006). Concrete microstructure, properties and materials. The McGraw-Hill Companies, Berkeley, USA.
Meng, Q.X., Lv, D., and Liu, Y. (2020). Mesoscale computational modeling of concrete-like particle-reinforced composites with non-convex aggregates. Computers & Structures, 240, 1-13.
Okan, Y., Molinari, J. (2017). A mesoscale fracture model for concrete. Cement and Concrete Research, 97, 84–94.
Scrivener, KL., Crumbie, AK., and Laugesen, P. (2004). The interfacial transition zone (ITZ) between cement paste and aggregate in concrete. Interface Science, 12, 411–421.
Song, Z., Lu, Y. (2012). Mesoscopic analysis of concrete under excessively high strain rate compression and implications on interpretation of test data. International Journal of Impact Engineering, 46, 41–55.
Thilakarathna, PSM. et al. (2020a). Mesoscale modelling of concrete – A review of geometry generation, placing algorithms, constitutive relations and applications. Engineering Fracture Mechanics, 231, 1-29.
Thilakarathna, PSM. et al. (2020b). Understanding fracture mechanism and behaviour of ultra-high strength concrete using mesoscale modelling. Engineering Fracture Mechanics, 234, 1-25.
van Mier, JGM. (2017). Concrete fracture: a multiscale approach. CRC Press, Boca Raton, USA.
Van Mier, JGM., Van Vliet, MRA. (2003). Influence of microstructure of concrete on size/scale effects in tensile fracture. Engineering Fracture Mechanics, 70, 2281–2306.
Wang, ZM., Kwan, AKH., and Chan, HC. (1999). Mesoscopic study of concrete I: Generation of random aggregate structure and finite element mesh. Computers & Structures, 70, 533–544.
Wittmann, FH., Roelfstra, PE., and Sadouki, H. (1985). Simulation and analysis of composite structures. Materials Science and Engineering, 68, 239–248.
Wriggers, P., Moftah, SO. (2006). Mesoscale models for concrete : Homogenisation and damage behaviour. Finite Elements in Analysis and Design, 42, 623–636.
Xu, J., Li, F. (2017). A meso-scale model for analyzing the chloride diffusion of concrete subjected to external stress. Construction and Building Materials, 130, 11–21.
Xu, W., Lv, Z., and Chen, H. (2013). Effects of particle size distribution, shape and volume fraction of aggregates on the wall effect of concrete via random sequential packing of polydispersed ellipsoidal particles. Physica A: Statistical Mechanics and its Applications, 392, 416–426.
Xu, WX., Chen, HS. (2013). Analytical and modeling investigations of volume fraction of interfacial layers around ellipsoidal aggregate particles in multiphase materials. Modelling and Simulation in Materials Science and Engineering, 21, 1-15.
Zhang, Y. et al. (2019). Validation and investigation on the mechanical behavior of concrete using a novel 3D mesoscale method. Materials, 12, 1-28.
Zhang, Z. et al. (2017). Three-dimensional mesoscale modelling of concrete composites by using random walking algorithm. Composites Science and Technology, 149, 235–245.
Zhou, R., Song, Z., and Lu, Y. (2017). 3D mesoscale finite element modelling of concrete. Computers & Structures, 192, 96–113.